Pattern formation in screened electrostatic fields: Growth in a channel and in two dimensions

J. Castellá and E. Louis
Departamento de Física Aplicada, Universidad de Alicante, Apartado 99, E-03080 Alicante, Spain

F. Guinea,* O. Pla, and L. M. Sander
Department of Physics, The University of Michigan, Ann Arbor Michigan 48109-1120
(Received 18 August 1992)

It is shown that screening greatly diversifies the type of patterns that can grow in an electrostatic field. Screening introduces a new length scale and a nontrivial dependence on the boundary conditions. Growing patterns can either have a fractal character (diffusion-limited-aggregation-like) at scales shorter than the screening length, be similar to the Eden model, or even be dense. A transition from dense to multibranched growth occurs at a point which depends on the potentials at the boundaries, the distance between them, and the screening length. Simulations are carried out in one dimension (growth in a channel) and in two dimensions (with different shapes for the outer electrode). The transition from dense to filamentary growth is also investigated by means of an analytical study of the instability, within a similar scheme to the one proposed by Mullins and Sekerka. The results are qualitatively similar for growth in one and two dimensions. Finally, it is shown that, before the transition (dense growth), the aggregate reproduces the shape of the outer electrode.

PACS numbers: 68.70.+w, 05.40.+j, 61.50.Cj

I. INTRODUCTION

The diffusion-limited-aggregation (DLA) [1, 2] and the dielectric breakdown (DB) [3] models have been very successful in illustrating the possibility of fractal growth [4] in Laplacian fields. Nature does offer, however, greater variety, in which both fractal and nonfractal patterns may grow. The dependence on the boundary conditions in the DB discussed in Ref. [5] illustrates this point: a change in the shape of electrodes induces drastic changes in the growing patterns which evolve into a rather dense multibranched structure with fractal dimension $D \sim 2$. Although several reasons have been suggested [5] to explain this dependence on the boundary conditions, among which we mention the existence of a threshold field and the internal resistance of the breakdown pattern (plasma channels in the case of a discharge in a gas), in very few instances have their effects been analyzed in any depth. Only the possibility of a different growth law, in which the growth rate is assumed to be proportional to a power η of the local field, different in general from unity, has been examined in detail in the DB context [3], utilized an equivalent approach in DLA [6], and used to explain patterns that are more diluted than DLA that may occur in Nature. Note, however, that there are microscopic reasons for expecting $\eta = 1$ in DB [7]. More recently, the possibility of a crossover from a DLA pattern to a more diluted one has also been investigated by using more complicated growth laws, both in the DB [8] and in the somewhat similar phenomena of mechanical breakdown [9–11]. The variety of structures further increases for the growth of metallic aggregates through electrochemical deposition (ECD). These may have a fractal character as in DLA, be dendritic crystals, or give rise to dense radial structures [12–18]. The stability of the latter has been ascribed to the finite resistivity of the aggregate [12], or to the anion migration between the electrodes [13, 16]. Also, a transition from a dense pattern to a more diluted branched structure has been observed [13, 19, 20] and referred to as the Hecker transition [20].

In this paper we investigate the effects of screening [21] on structures growing in electrostatic fields. The origin of screening might lie on the presence of free charges in the cases of ECD and DB. From elementary considerations of thermal equilibrium, the Debye-Hückel theory deduces the existence of a screening length which depends on the total density of charges and the temperature [22]. The same situation may arise in DLA; in this case screening might be due to the presence of sinks (screening) or an ambient density of particles (antiscreening), see for instance Ref. [23]. We have carried out numerical simulations and an analytical study along the lines proposed by Mullins and Sekerka [24]. The results show that screening leads to a rich variety of patterns. It introduces a new length scale and a nontrivial dependence on the boundary conditions which, as discussed below, is responsible for a transition that resembles the Hecker transition. Patterns may have a fractal character at shorter scales than the screening length, and be Eden-like or grow dense at larger scales. The above-mentioned transition (from dense to multibranched growth) is shown to occur at a point that depends on the potentials at the two boundaries, the distance between them, and the screening length.

II. MODEL AND NUMERICAL METHODS

We concentrate on the DB model [3]. In that model a breakdown pattern is allowed to grow in a dielectric medium placed between two electrodes at different potentials. The aggregate is assumed to be a perfect conductor, and, thus, at constant potential, whereas fields in the dielectric follow the Laplace equation. To account for screening we replace the Laplace equation by

$$\nabla^2\phi = \lambda^2\phi, \tag{1}$$

where λ^{-1} is the screening length. The Debye-Hückel theory imples that $\lambda^2 = 4\pi e^2\rho/k_BT$, where e is the charge of the ions, ρ its (three-dimensional) density, k_B the Boltzmann constant, and T the temperature. In the following, we will assume that λ^{-1} is a length intermediate between atomic scales and the macroscopic dimension of the container. However, for many ECD experiments, λ^{-1} is only a few angstroms so that the theory in this paper is not directly applicable.

Antiscreening would correspond to a minus sign on the right-hand side of Eq. (1). Its effects will be briefly discussed at the end of Sec. III A. We shall consider a planar geometry (growth in a channel) and growth in two dimensions.

To originate an aggregate Eq. (1) implemented on a lattice was solved iteratively. The potential was fixed at the outer (ϕ^o) and the inner (ϕ^i) electrodes; the latter also gave the potential at the aggregate, assumed to be a perfect metal at constant potential. In the following we shall consider λ and the potentials ϕ^o and ϕ^i as tunable positive parameters. In an actual experiment, ϕ^o and ϕ^i will be determined by the external circuit, which fixes the potential drop, and by the requirement of charge conservation. As a consequence Eq. (1) is not gauge invariant and it only has physical meaning for the gauge implied by the choice of potentials just mentioned. We also note that care should be taken that the linearization implicit in the Debye-Hückel theory can be applied.

Once the system has been relaxed, growth takes place in the nearest neighbors of the aggregate with probability proportional to the absolute value of the electric field at these points; and the system is again relaxed.

Numerical simulations were carried out on samples of the square lattice of sizes 100×200 for the case of growth in a channel, and on samples of the square and the triangular lattices with radii up to 100, for two-dimensional (2D) growth. In the former case the boundaries along the longest direction were taken as the electrodes, whereas periodic boundary conditions were used in the shorter direction. On the other hand, simulations in two-dimensions were carried out for a variety of shapes of the outer electrode, in particular circular, triangular, and square electrodes were considered. It has to be remarked that screening can strongly decrease the potential at the surface, changing quickly (see Fig. 1) as the pattern evolves, thus the error used to stop the iteration process should be decreased or increased properly. Our criterion was that the maximum error at each node was less than 1% the average value of the electric field at the boundary of the pattern (the relative error is thus 0.01,

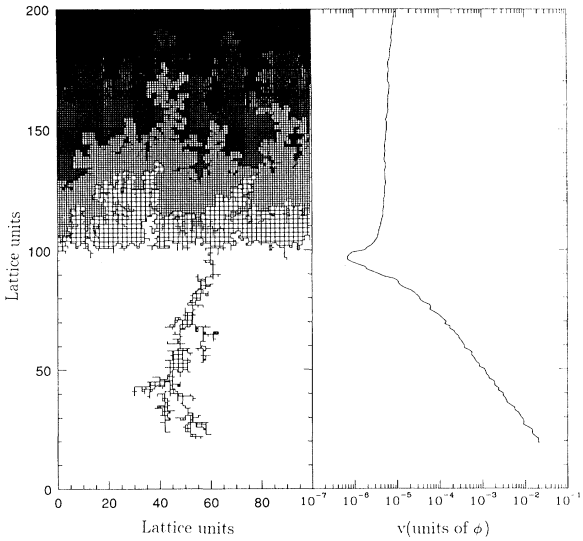

FIG. 1. Growth in a channel: The left graph shows in decreasing intensity of shading the shape of the advancing front as the aggregate grows. Each change in intensity corresponds to 2433 particles more. In the right graph, the growth velocity (average of the absolute value of the electric field at the surface of the aggregate) is plotted. The parameters are $\lambda^{-1} = 10$, $\phi^o = 1$, and $\phi^i = 10^{-4}$.

which is accurate enough if we consider the randomness in the election of the new attached particle). This gave around 50 iterations to relax the electrostatic field. This criterion was also checked for several realizations by solving the discretized equations by conjugate gradients, giving the same quantitaive results as the method exposed above.

III. ANALYSIS OF THE INSTABILITY

To get a qualitative idea of the effects of screening on the growth process, we first analyze the stability of a slightly deformed smooth surface by following the treatment first discussed in Ref. [24]. We discuss both the stability of a flat surface growing in a channel and that of a circle growing in a circular cell.

A. Growth in a channel

Let us consider a flat boundary, say $y = y^i$, growing in the y direction between two electrodes at potentials ϕ^o and ϕ^i, respectively, and itself at a constant potential ϕ^i. We then deform the surface as $y^m = y^i + \delta\cos(mx)$, δ being very small. In the screened case the potential takes the form (setting $\phi = \phi^i$ at $y = y^m$)

$$\phi(x,y) = \phi_0(y) + E_0(y^i)\delta\exp[-\sqrt{\lambda^2+m^2}(y-y^i)]\cos(mx), \tag{2}$$

where

$$\phi_0(y) = \frac{\phi^o \sinh[\lambda(y - y^i)] + \phi^i \sinh[\lambda(y^o - y)]}{\sinh[\lambda(y^o - y^i)]}, \quad (3)$$

y^o is the length of the cell in the growth direction (y), and $E_0(y^i)$ is the electric field at the flat surface ($y = y^i$),

$$E_0(y^i) = \frac{\phi^i \cosh[\lambda(y^o - y^i)] - \phi^o}{\sinh[\lambda(y^o - y^i)]}\lambda. \quad (4)$$

Then, assuming that the growth rate v is proportional to the absolute value of the field at the surface of the aggregate and writing $v = \dot{y}^i + \dot{\delta}\cos(mx)$, we find for the ratio between the instantaneous rates of growth of the perturbation (δ) and that of the flat surface (y^i) the following expression [25]:

$$\alpha_m = \frac{\dot{\delta}/\delta}{\dot{y}^i/y^i} = \left(\sqrt{\lambda^2 + m^2} - \frac{\lambda^2 \phi^i}{E_0(y^i)}\right) y^i. \quad (5)$$

In the case of no screening Eq. (5) reduces to the known result $\alpha_m = my^i$. When screening is present the instantaneous growth rate depends on the potentials at the electrodes, the gap between them ($y^o - y^i$), and the screening length (λ^{-1}). Two cases should be distinguished. For $\phi^o < \phi^i$, the field at the surface of the aggregate has the same polarization of the electrodes for all values of y^i [for which $E_0(y^i) > 0$]. Thus, the second term on the right hand side of Eq. (5) is always negative, decreasing in absolute value as the pattern evolves. Consequently, the effect of screening will be to create dense structures which become more dilute while growing, but still resemble the Eden model.

More interesting changes are found in the case of $\phi^o > \phi^i$. In this case the most interesting feature is the possibility that $E_0(y^i)$ vanishes. We should note that this corresponds to a breakdown of overall charge neutrality: the screening charge at both electrodes is of the same sign. In many cases this effect is excluded on physical grounds. This vanishing of the electric field occurs at a critical length of the aggregate y_c^i, given by

$$\cosh[\lambda(y^o - y_c^i)] = \frac{\phi^o}{\phi^i}. \quad (6)$$

For $y^o \gg y^i$ and provided that $\phi^o/\phi^i < \cosh[\lambda y^o]$, $E_0(y^i)$ is opposite to the polarization of the electrodes ($E_0(y^i) > 0$). It goes to zero at a given value of the length of the aggregate (y_c^i) and, beyond this point, it is always negative. As a consequence, the second term in α_m is initially negative, as in the previous case, but now it increases in absolute value. As the length of the aggregate increases, and the zero of the denominator is approached, the screening term slows down the perturbations of every wavelength, and the growth rate is reduced. The α_m will vanish and become negative at different values of y^i (Fig. 2). A wavelength-selection mechanism will thus take place in such a way that the minimum m that a perturbation should have in order to be amplified will increase with y^i. As a result the number of branches across the width will increase and the surface of the aggregate will become gradually fatter. Then, at a distance which depends on the parameters of the problem, (ϕ^o, ϕ^i, and

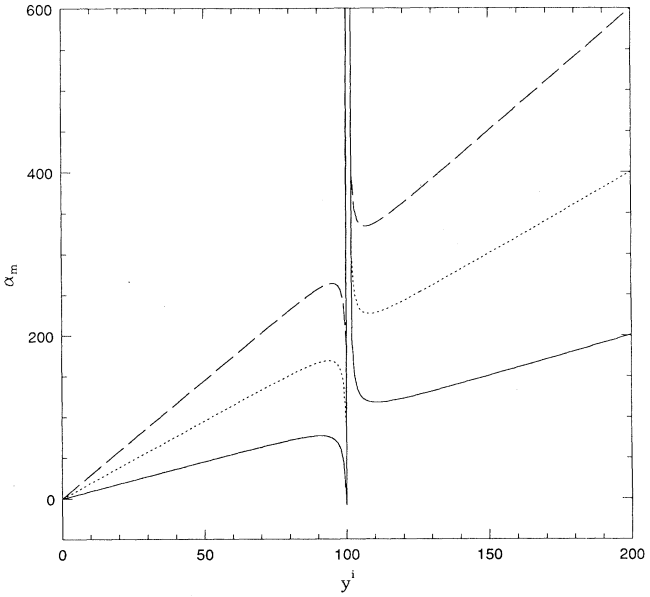

FIG. 2. The instability of the front (α_m) as it evolves. The parameters are those of Fig. 1. Different values of m are shown: 1 (continuous line), 2 (dotted line), and 3 (dashed line).

the screening length λ^{-1}) $E_0(y^i)$ vanishes and all α_m will change from $-\infty$ to $+\infty$. A flat front will result. Beyond this point (y_c^i) all wavelengths become unstable. Once a sharp tip develops, it will be amplified.

This behavior is a consequence of the potential and its associated charge distribution. Before the transition, there is a small screening layer near the growing electrode. In the intermediate region the potential decreases to a value close to zero, to rise again near the external electrodes. Beyond the transition these two layers merge and the potential increases monotonically between the aggregate and the outer electrode. It is worth noticing that these results are not necessarily linked to the model discussed in Sec. II, and may have a more general character as demostrated in the Appendix for the case of a dielectric having a constant density of free charges.

We turn now to comment briefly on the effects of antiscreening. As remarked above this would correspond to the presence of an ambient (density of sources) of particles in DLA, and might be relevant in ECD as far as ions could be generated anywhere between the electrodes. In this case all magnitudes are oscillating functions. In particular, the field at the surface of the aggregate is given by

$$E_0(y^i) = \frac{\phi^i \cos[\lambda(y^o - y^i)] - \phi^o}{\sin[\lambda(y^o - y^i)]}\lambda. \quad (7)$$

Now the field only vanishes when $\phi^i > \phi^o$ and this may occur for several sizes of the aggregate. A procedure similar to that described above gives the following expression for the ratio between the instantaneous growth rates:

$$\alpha_m = \left(\Theta(m^2-\lambda^2)\sqrt{m^2-\lambda^2} + \frac{\lambda^2\phi^i}{E_0(y^i)}\right) y^i, \qquad (8)$$

where Θ is the step function. The oscillatory character of α_m originates a behavior which is even richer than that found in the screening case. For instance, transition(s) similar to that described above may also take place, although in this case they can only occur for $\phi^i > \phi^o$.

B. Growth in two dimensions

We now consider a perfectly metallic aggregate of circular shape, i.e., a disc of radius r^i at constant potential ϕ^i, growing in a dielectric medium, and an outer electrode also circular ($r = r^o > r^i$) at potential ϕ^o. Here we shall only discuss the case of screening and $\phi^o > \phi^i$. The field at a point $z = \lambda r$ in the dielectric takes the form

$$E_0(z) = \frac{\phi^i[K_1(z)I_0(z^o) + I_1(z)K_0(z^o)] - \phi^o[K_0(z^i)I_1(z) + I_0(z^i)K_1(z)]}{I_0(z^o)K_0(z^i) - I_0(z^i)K_0(z^o)}\lambda, \qquad (9)$$

where $z^{i,o} = \lambda r^{i,o}$ and I_n and K_n are the modified Bessel functions. As in the one-dimensional (1D) case, the field is first (small z) opposite to the polarization of the outer electrodes and goes through zero at a point in between the aggregate surface and the outer electrode. Beyond this point the field has, for all z, the same polarization of the electrodes. Again, the field at the surface of the aggregate $E_0(z^i)$ vanishes at a point z_c^i given by

$$\frac{[K_1(z_c^i)I_0(z^o) + I_1(z_c^i)K_0(z^o)]}{[K_0(z_c^i)I_1(z_c^i) + I_0(z_c^i)K_1(z_c^i)]} = \frac{\phi^o}{\phi^i}. \qquad (10)$$

As found in the one-dimensional case this behavior of the field determines the stability of the circularly shaped aggregate. To carry out the stability analysis we deform the circular surface of the aggregate as $z_n = z^i + \lambda\delta\cos(n\theta)$, where δ is small. The result for the ratio between the instantaneous rates of growth of the perturbation (δ) and that of the disc (z^i) is

$$\alpha_n = \frac{\dot{\delta}/\delta}{\dot{z}^i/z^i} = n - 1 + z^i\left(\frac{K_{n-1}(z^i)}{K_n(z^i)} - \frac{\lambda\phi^i}{E(z^i)}\right). \qquad (11)$$

The behavior of α_n is similar to that obtained in the previous case. Again the α_n vanish at different values of z^i, favoring dense growth. At the point where $E(z)$ vanish, α_n for all n goes to infinity, and the transition from dense to ramified growth takes place. The discussion that follows Eq. (5) is also valid here.

IV. NUMERICAL SIMULATIONS

The results of the numerical simulations carried out in this work, illustrated in Figs. 1 and 3–7, fully coincide with the predictions of the analysis of the instability discussed in the preceeding section. We first comment on the results for the one-dimensional case. Figure 1 shows the aggregate at different stages during the growth process. As predicted, growth sharply changes from dense to ramified. We have calculated, from Eq. (6), the length at which the transition should occur for the parameters of the figure, resulting $l \sim 101$, in excellent agreement with the numerical results. It should be pointed out that this is a remarkable demonstration of the validity of the analysis first suggested by Mullins and Sekerka [24]. The occurrence of the transition in a wide range of the parameters is further illustrated in Fig. 3, again it takes place at the points predicted by the analytical study. In Fig. 1 we have also plotted the average growth speed, that is the average of the absolute value of the field at the aggregate surface. We note that, as discussed above, the velocity nearly vanishes at the transition. Finally we refer to the width of the branches that grow beyond the transition point. As shown in Fig. 3 its width increases as λ decreases, being DLA-like at scales shorter than the screening length λ^{-1}. It is remarkable that screening produces dilute patterns without using a growth rate proportional to a power η of the electric field different from unity.

We have also considered under which conditions several branches may develop. Screening reduces the range of the interaction, and, therefore, should pose no problems to the growth of parallel branches. In the simulations outlined above, however, particles are added one at a time. This effect induces a sharp threshold in the velocity of growth, so that points where the field exceed this threshold will grow and not others. Since the fields in this screened situation have an exponential dependence on the separation between electrodes, this artificial cutoff prevents most of the front from growing. To overcome this difficulty we have considered a front of particles that may attach stochastically at different sites without rearranging the potential in the dielectric. The results are illustrated in Fig. 4. As expected, several parallel branches grow simultaneously.

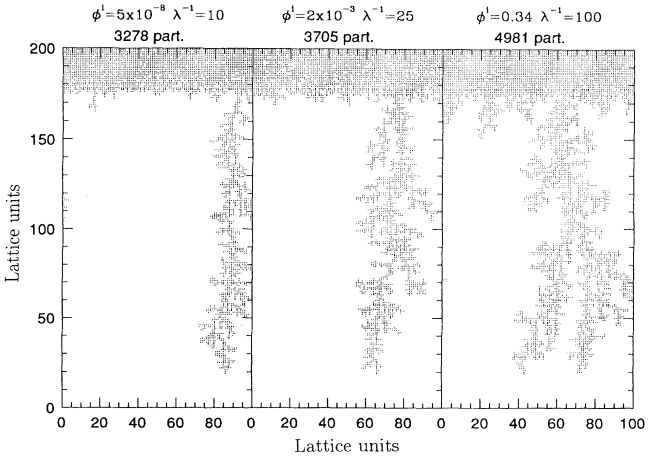

FIG. 3. Growth in a channel: Different patterns grown with $\phi^o = 1$ and several values of λ^{-1} and ϕ^i.

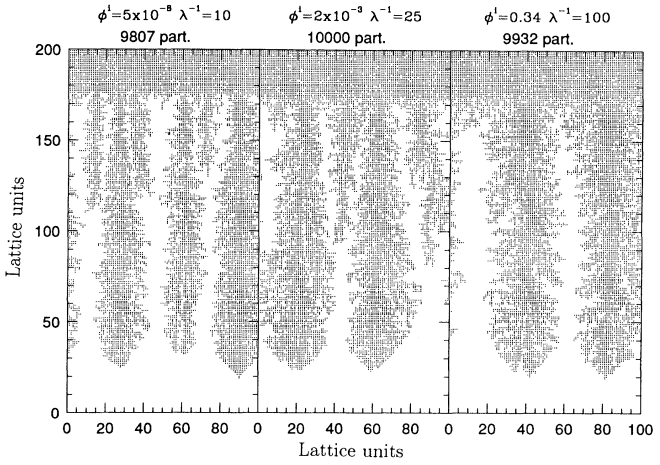

FIG. 4. Same as Fig. 3 but simultaneously attaching 50 particles at each step.

Figures 5–7 show some patterns obtained in the two-dimensional case. The transition is also well defined, due to the choice of parameters. The most outstanding feature of the aggregates shown in Fig. 5 is that their shape before the transition mimics the shape of the outer electrode. This is a consequence of screening. In the case of no screening aggregates grow isotropically and reflect the shape of the outer electrode only when they get very close to it. This effect could be easily understood by looking at the equipotential lines between two electrodes at different potentials, the inner a single point at the center and the outer of an arbitrary shape. In the unscreened case the equipotential lines are almost circular up to very near the outer electrode. In the presence of screening and due to the much shorter range of the in-

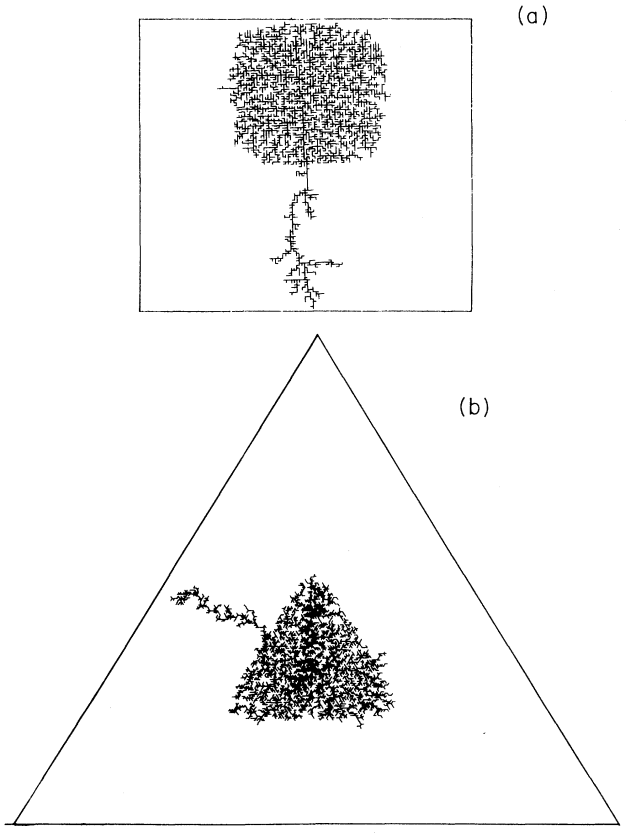

FIG. 5. Growth in two dimensions for $\lambda^{-1} = 10$ and $\phi^o = 1$. Patterns grown with a square electrode in a square lattice ($\phi^i = 0.002$) and a triangular electrode in a triangular lattice ($\phi^i = 0.062$) are shown. In both cases $r_c^i = 25$.

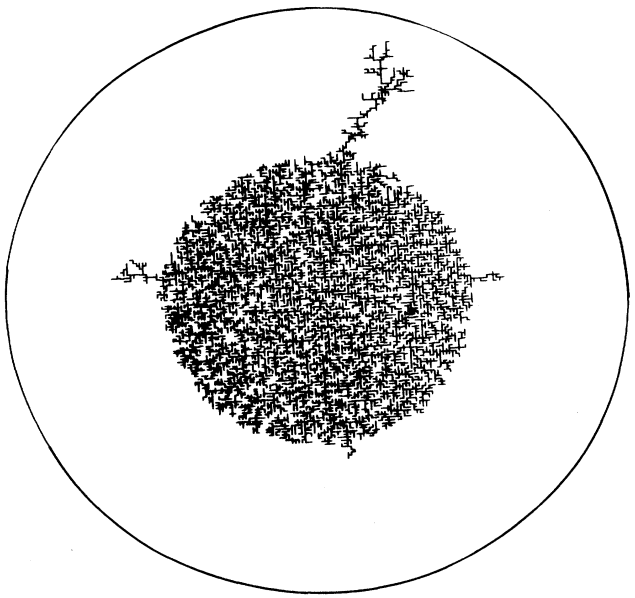

FIG. 6. Growth in a square lattice with a circular electrode. $\lambda^{-1} = 10$, $\phi^o = 1$, and $\phi^i = 0.9$ ($r_c^i = 50$).

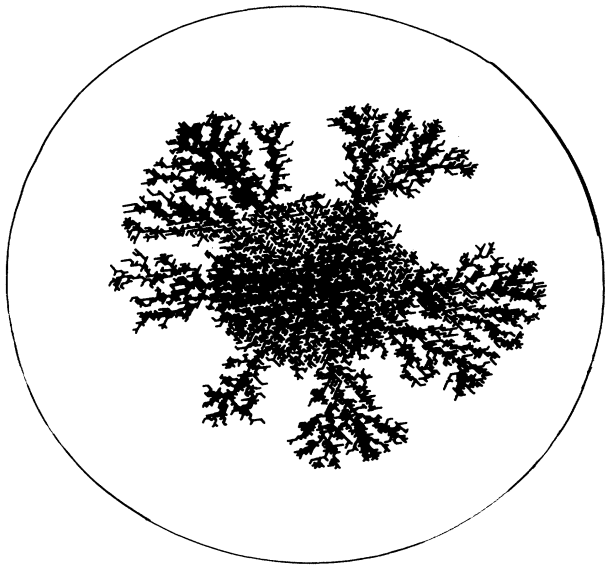

FIG. 7. Growth in a triangular lattice: Circular electrode, $\lambda^{-1} = 10$, $\phi^o = 1$, and $\phi^i = 0.006$. 75% of the pixels contained in the perimeter of the circumference corresponding to the average radius of the aggregate were attached at each step.

teraction, the equipotential lines reflect the shape of the outer electrode even far from it, as only the zones that are at the shortest distances contribute appreciably to the local potential. Although this explanation is rather obvious, we have checked that the results of Fig. 6 are not lattice effects by considering the case of a triangular electrode in the square lattice and vice versa. The results demonstrate that the shape of the aggregate only depends on the shape of the electrode and not on the choice of a particular lattice. Finally we note that the effect of allowing a front of particles to stick simultaneously to the aggregate surface is similar to that found for growth in a channel (Fig. 7). In this case we have kept constant the flux of particles (instead of the number as done in the 1D case).

V. DISCUSSION AND CONCLUDING REMARKS

At first glance the transition mentioned above shares many common features with the so-called Hecker transition [20] observed in ECD. In both cases dense and filamentary patterns develop at different times. The complexity of the real experiments greatly exceeds the simple model described here, and, presumably, other effects like those derived from the propagation of fronts of charged impurities towards the cathode, as discussed in Refs. [13] and [16], shall also be taken into account in a complete theory. However, some aspects of the Hecker transition are similar to those of the present model. The transition described before is characterized by a change in the sign of the electrostatic field at the surface of the aggregate. If that takes place in the Hecker transition, a change in the charge of the chemical species being accumulated near the cathode should also take place. This conclusion seems reminiscent of experimental findings, where a change in color associated with a change in the material being deposited (metal oxides are replaced by metallic ions in going through the transition) has been reported. A similar change in color of the solution has been identified as a change in the pH, which occurs simultaneously with the transition. Moreover, assuming the screening length to be much smaller than the size of the cell, the occurrence of the transition in the center of the cell, as observed experimentally, requires that $\phi^o \gg \phi^i$ (Fig. 1). This implies that, before the transition, the field near the aggregate will be opposite to the polarization of the electrodes (as outlined above), although very low. Hence this electrostatic barrier can easily be overcome by cations through a diffusive process. However, we recall that, as we pointed out above, our model is not directly applicable to this experiment.

In conclusion, we have presented an investigation of the effects of screening on growth phenomena in screened electrostatic fields. Screening strongly increases the diversity of patterns, giving rise, under certain conditions and in a very simple way, to a transition from dense to multibranched growth. On the other hand, the shape of the aggregate before this transition closely reflects that of the outer electrode. Some of these features are similar to those of the so-called Hecker transition observed in ECD.

ACKNOWLEDGMENTS

We are grateful to A. Aldaz, J.A. Vallés-Abarca, and J. Vázquez for useful suggestions and comments. Two of us (J.C. and O.P.) wish to acknowledge financial support from the Ministerio de Educación y Ciencia, Spain. L.M.S. is supported by the U.S. NSF Grant No. DMR 91-17249, and F.G., E.L., and O.P. by the Spanish CICYT Grant No. MAT91-0905-C02-02.

APPENDIX

Here we consider the case of a dielectric medium that, instead of being described by Eq. (1), has a constant density of free charges. The Poisson equation can now be written as

$$\nabla^2\phi = \rho_0. \tag{A1}$$

As in Sec. III A we consider a flat boundary, growing in the y direction between two electrodes (outer and inner) at potentials ϕ^o and ϕ^i, respectively, and itself at a constant potential ϕ^i. The potential at the deformed surface $y^m = y^i + \delta\cos(mx)$, now takes the form

$$\phi(x,y) = \phi_0(y) + E_0(y^i)\delta\exp[-m(y-y^i)]\cos(mx), \tag{A2}$$

where

$$\phi_0(y) = \tfrac{1}{2}\rho_0[y^o y^i - (y^o + y^i)y + y^2] + \phi^i + \frac{\phi^o - \phi^i}{y^o - y^i}(y - y^i) \tag{A3}$$

and $E_0(y^i)$ is the electric field at the flat surface ($y = y^i$),

$$E_0(y^i) = \tfrac{1}{2}\rho_0(y^o - y^i) - \frac{\phi^o - \phi^i}{y^o - y^i}. \tag{A4}$$

Finally, the result for the ratio between the instantaneous rates of growth of the perturbation (δ) and that of the flat surface (y^i) is

$$\alpha_m = \left(m - \frac{\rho_0}{E_0(y^i)}\right) y^i. \tag{A5}$$

The behavior of α_m is very similar to that obtained for the model of Sec. II. It reproduces all the results discussed in previous sections, including the transition from dense to ramified growth. Thus it can be concluded that the present results are not necessarily restricted to systems described by Eq. (1).

It is interesting to note that this model is similar to the one recently proposed by La Roche *et al.* [23] to explain the patterns that grow in a variable Hele-Shaw cell. Sources of particles such as those considered in [23] would correspond to $\rho_0 < 0$.

* Permanent address: Instituto de Ciencia de Materiales (CSIC), Facultad de Ciencias C-XII, Cantoblanco, E-28049 Madrid, Spain.

[1] T. A. Witten and L. M. Sander, Phys. Rev. Lett. **47**, 1400 (1981).
[2] T. A. Witten and L. M. Sander, Phys. Rev. B **27**, 2586 (1983).
[3] L. Niemeyer, L. Pietronero, and H. J. Wiesmann, Phys. Rev. Lett. **52**, 1033 (1984).
[4] B.B. Mandelbrot, *Fractal Geometry of Nature* (Freeman, New York, 1982).
[5] L. Niemeyer, L. Pietronero, and H. J. Wiesmann, Phys. Rev. Lett. **57**, 650 (1986).
[6] J. H. Kaufman, G. M. Dimino, and P. Meakin, Physica A **157**, 656 (1989).
[7] I. Gallimberti, J. Phys. (Paris) Colloq. **40**, C7-1936 (1979).
[8] E. Arian, P. Alstrom, A. Aharony, and H. E. Stanley, Phys. Rev. Lett. **63**, 3670 (1990).
[9] E. Louis and F. Guinea, Europhys. Lett. **3**, 871 (1987).
[10] E. Louis and F. Guinea, Physica D **38**, 235 (1989).
[11] O. Pla, F. Guinea, E. Louis, G. Li, L. M. Sander, H. Yan, and P.Meakin, Phys. Rev. A **42**, 3670 (1990).
[12] D. G. Grier, D. A. Kessler, and L. M. Sander, Phys. Rev. Lett. **59**, 2315 (1987).
[13] V. Fleury, M. Rosso, and J.-N. Chazalviel, Phys. Rev. B **43**, 690 (1991); V. Fleury, M. Rosso, J.-N. Chazalviel, and B. Sapoval, *ibid.* **44**, 6693 (1991).
[14] P. Garik, D. Barkley, E. Ben-Jacob, E. Bochner, N. Broxholm, B. Miller, B. Orr, and R. Zamir, Phys. Rev. Lett. **62**, 2703 (1989).
[15] V. Fleury, J.-N. Chazalviel, M. Rosso, and B. Sapoval, J. Electroanal. Chem. **290**, 249 (1990).
[16] J. R. Melrose, D. B. Hibbert, and R. C. Ball, Phys. Rev. Lett. **65**, 3009 (1990).
[17] F. Sagués, F. Mas, and J.M. Costa, J. Electranal. Chem. **278**, 351 (1990); P.P. Trigueros, J. Claret, F. Mas, and F. Sagués, *ibid.* **312**, 219 (1991); F. Mas and F. Sagués, Europhys. Lett. **17**, 541 (1992).
[18] J.-N. Chazaviel, Phys. Rev. A **42**, 7355 (1990).
[19] N. Hecker, D. G. Grier and L. M. Sander, in *Fractal Aspects Of Materials*, edited by R. B. Laibowitz, B. B. Mandelbrot, and D. E. Passoja (Materials Research Society, University Park, PA, 1985).
[20] L. M. Sander, in *The Physics of Structure Formation*, edited by W. Guttinger and G. Dangelmayr (Springer-Verlag, Berlin, 1987).
[21] E. Louis, F. Guinea, O. Pla, and L. M. Sander, Phys. Rev. Lett. **68**, 209 (1992).
[22] W. J. Moore, *Physical Chemistry* (Prentice-Hall, Englewood Cliffs, NJ, 1962), Vol. 1.
[23] H. La Roche, J.F. Fernández, M. Octavio, A.G. Loeser, and C.J. Lobb, Phys. Rev. A **44**, R6185 (1991).
[24] W. W. Mullins and R. F. Sekerka, J. Appl. Phys. **34**, 323 (1963).
[25] In Ref. [21] α_m was incorrectly written in terms of the absolute value of the right-hand side of Eq. (5). Note that the fact that the value of α_m can be negative does not mean that the aggregate should stop growing. The total growth speed which is given by $\dot{y}^i + \dot{\delta}\cos(mx)$ is assumed to be always positive (proportional to the absolute value of the local field).